# INTERNATIONAL SOCIETY FOR SOIL MECHANICS AND GEOTECHNICAL ENGINEERING



This paper was downloaded from the Online Library of the International Society for Soil Mechanics and Geotechnical Engineering (ISSMGE). The library is available here:

# https://www.issmge.org/publications/online-library

This is an open-access database that archives thousands of papers published under the Auspices of the ISSMGE and maintained by the Innovation and Development Committee of ISSMGE.

The paper was published in the proceedings of the 20<sup>th</sup> International Conference on Soil Mechanics and Geotechnical Engineering and was edited by Mizanur Rahman and Mark Jaksa. The conference was held from May 1<sup>st</sup> to May 5<sup>th</sup> 2022 in Sydney, Australia.

# Punching settlement of raft-pile foundation under cyclic loading

# Règlement de poinçon de la fondation de radeau-pile sous le chargement cyclique

# T. Mirsayapov Ilizar

KSUAE, head of department, Russia, mirsayapov1@mail.ru

ABSTRACT: The settlement of raft-pile foundation under cyclic loading consists of three components: the settlement of the conditional foundation, the settlement due to compression of the pile and punching settlement. The punching settlement of raft-pile foundation significantly changes the distribution of loads on the piles especially on the outer and corner ones, which are overloaded. In this article, this process is considered in 3D, taking into account the joint deformation of all elements of the system "pile cap - piles - soil between piles - soil below toe". The redistribution of efforts between the elements of the system during cyclic loading is taken into account due to the occurrence of deformations of soil, pile cap and piles in the related conditions. The settlement of the raft-pile foundation is determined for the stage when tangential stresses along the side surface are absent in the upper and middle part of the pile as a result of reaching the ultimate shear resistance. The soil is pushed through under the toe when the stress under the pile toe and under the raft exceeds the fatigue strength and maximum deformations of the soil under triaxial cyclic compression. Comparison of the calculation results for the proposed model with experimental studies showed good convergence.

RÉSUMÉ: Le règlement de la fondation radeau-pieux sous chargement cyclique se compose de trois composants: le règlement de la fondation conditionnelle, le règlement dû à la compression de la pile et le règlement de poinçonnage. Le règlement de poinçonnage de la fondation sur pieux de radeau modifie considérablement la répartition des charges sur les pieux, en particulier sur ceux extérieurs et d'angle, qui sont surchargés. Dans cet article, ce processus est considéré en 3D, en tenant compte de la déformation conjointe de tous les éléments du système "semelle sur pieux - pieux - sol entre pieux - sol sous la pointe". La redistribution des efforts entre les éléments du système pendant le chargement cyclique est prise en compte en raison de l'apparition de déformations du sol, du chapeau de pile et des pieux dans les conditions connexes. Le règlement de la fondation radeau-pile est déterminé pour l'étape où les contraintes tangentielles le long de la surface latérale sont absentes dans la partie supérieure et moyenne de la pile en raison de l'atteinte de la résistance au cisaillement ultime. Le sol est poussé sous la pointe lorsque la contrainte sous la pointe de la pile et sous le radeau dépasse la résistance à la fatigue et les déformations maximales du sol sous compression cyclique triaxiale. La comparaison des résultats de calcul pour le modèle proposé avec les études expérimentales a montré une bonne convergence.

KEYWORDS: raft-pile foundation, cyclic load, piles, pile cap, soil, stress, triaxial loading, punching, settlement, cohesion.

## 1 INTRODUCTION.

The settlement of the raft-pile foundation significantly changes the distribution of loads on the piles in the raft-pile foundation, especially on the outer and corner ones (Bokov & Fedorovskii 2018, 2019), which are overloaded and therefore can settle without increasing the load on them, that is, go to the limit state on the soil below the toe (if the pile is not rigidly connected with the pile cap) and under the pile cap at the same time (if the pile is rigidly connected with the pile cap). Such piles are called "creeping". Foundations in which some or all piles are "creeping" can be the optimal solution to minimize the number of piles (Bokov & Fedorovskii 2018, 2019, Harichkin et al. 2018, Travush et al. 2019). The regularities of pile foundation settlements under cyclic loading are insufficiently studied (Ni et al. 2015, Lei et al. 2016, Shulyatev 2016, Hirai 2017, Ren et al. 2018).

# 2 MATERIALS AND METHODS

The creep of the outer and corner piles significantly changes the load distribution on all the piles of the raft-pile foundation. This process is considered in a spatial formulation, taking into account the joint deformation of all elements of the system "pile cap - piles - soil of the piles space - soil below the toe of the pile" due to the rigid connection of the pile and the pile cap (Fig. 1).

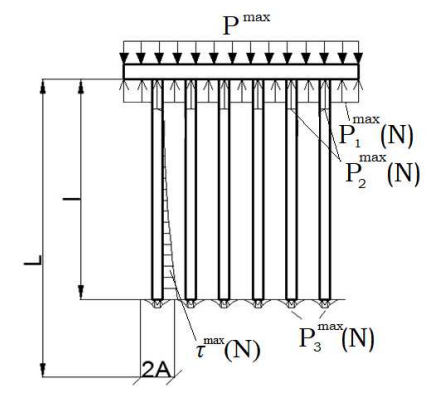


Figure 1. Design scheme of interaction of raft-pile foundation with the soil

The redistribution of forces between the system elements during cyclic loading due to the joint deformation of the pile cap, piles, the soil of the inter-pile space and the soil below the toe of the pile are taking into account. The stresses in certain specific zones of the system are determined by jointly solving 4 quasi-static equations (1-4), and the results of Z. G. Ter-Martirosyan's study for the case of static loading are taken as the basis (Ter-Martirosyan & Sidorov 2010):

$$p \cdot AB = p_2(N) \cdot ab + p_1(N)(AB - ab) \tag{1}$$

$$p_2(N) \cdot ab = p_3(N) \cdot ab - 4(a+b) \cdot l \cdot \frac{\tau_0(N)}{\alpha} \cdot e^{-\alpha l} + (a+b) \cdot l \cdot \frac{\tau_0(N)}{\alpha}$$
 (2)

$$\frac{\frac{p_1(N) \cdot \beta_{gr} \cdot L}{E_{gr}(N)} \left(1 - \frac{l}{L}\right) + \frac{k_1 \cdot \tau_0(N) \cdot (A - a)}{3G_{gr}(N)} + \frac{k_2 \cdot \tau_0(N) \cdot (B - b)}{3G_{gr}(N)} = \frac{\omega \cdot a \cdot p_3(N) \cdot (1 - v_{gr}) \cdot k(l)}{G_{gr}(N)}$$

$$(3)$$

$$\frac{p_{1}(N) \cdot \beta_{gr} \cdot L}{E_{gr}(N)} + \frac{k_{1} \cdot \tau_{0}(N) \cdot e^{-al} \cdot (A-a)}{3G_{gr}(N)} + \frac{k_{2} \cdot \tau_{0}(N) \cdot e^{-al} \cdot (B-b)}{3G_{gr}(N)} =$$

$$\frac{\tau_{0}(N)(a+b)l}{aba \cdot E_{p}} + \frac{\tau_{0}(N)(a+b)e^{-al}}{aba^{2} \cdot E_{p}} + \frac{p_{3}(N) \cdot l}{E_{p}} +$$

$$\frac{\omega \cdot a \cdot p_{3}(N) \cdot (1-v_{gr}) \cdot k(l)}{G_{gr}(N)} - \frac{\tau_{0}(N)(a+b)}{aba^{2} \cdot E_{p}}$$

$$(4)$$

where

$$p_1^{\max}(N) = \sigma_{gr1}^{\max}(N) - \Delta\sigma_{gr}(N)$$
 (5)

$$p_2^{\max}(N) = \sigma_p^{\max}(N) + \Delta \sigma_p(N) \tag{6}$$

$$p_3^{\max}(N) = \sigma_{qr3}^{\max}(N) - \Delta\sigma_{qr}(N) \tag{7}$$

$$\tau^{\max}(N) = \tau_0(N) \cdot e^{-\alpha z} \tag{8}$$

$$\tau(z) = \tau_0 \cdot e^{-\alpha z} \tag{9}$$

$$\alpha = \frac{5}{l} \tag{10}$$

where  $p_1^{\max}(N)$  is the stress in the soil under the pile cap,  $p_2^{\max}(N)$  is the stress in the head of pile,  $p_3^{\max}(N)$  is the stress in the soil under the pile toe,  $\tau^{\max}(N)$  is the maximal shear stress on the pile side surface.

Stresses in certain zones of the system are determined by solving the above (1-4) equations, depending on the number of loading cycles and parameters of cyclic loading. This method takes into account the change in the zone of ultimate equilibrium along the side surface of the piles, depending on the coordinate of the intersection point of the plots of the mobilized tangent stress  $\tau^{max}$  (N) and the ultimate tangent stress  $\tau^*$  (N) (Fig. 2).

The limit values of tangential stresses in the soil along piles are calculated based on the Mohr–Coulomb law:

$$\tau^*(N) = \gamma z \cdot \tan \varphi(N) + C(N) + \Delta \sigma_r^{\text{MOII}} \cdot \tan \varphi(N)$$
 (11)

where C(N) is the cohesion between soil particles under cyclic loading conditions;  $\Delta \sigma_x^{\text{gon}} = \sigma_{\bar{c}p} \cdot \text{tg } \varphi(N)$  is the additional horizontal pressure on the pile from the soil due to joint deformation of the system;  $\sigma_{\bar{c}p}$  is the stresses in the soil between piles from the action of the pile cap;  $\varphi(N)$  is the friction angle of soil under cyclic loading.

The cohesion between soil particles under cyclic loading is calculated based on the results of the author's research (Mirsayapov et al 2012, Mirsayapov & Shakirov 2016):

$$c(N) = c_0 \cdot m(t_1 \tau_1) \cdot \lambda(t_1 \tau_1) \cdot \sqrt{\frac{k(\tau_1)}{k(t)} + \frac{1}{1 + k(\tau_1)} \cdot c(t_1 \tau)}$$
(12)

where C<sub>0</sub> is the cohesion between the soil particles under short-term static loading.

Tangential stresses are calculated as follows:

$$\tau_0^{\max}(N) = \frac{a \cdot b(p_3(N) - p_2(N))}{(a + b) \cdot l \cdot \frac{1}{a^*} (4e^{-al} - 1)}$$
(13)

The equations (1-4) must be solved for each cycle, taking into account changes in all system parameters due to the

redistribution of forces between the pile cap, piles and soil during cyclic loading, including changes in the zone of limiting equilibrium in the soil between piles (Fig. 2).

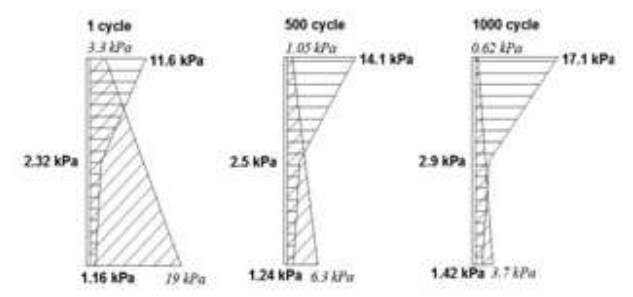


Figure 2. Plots of the mobilized tangential stress and the ultimate tangential stress in the soil along the piles.

Stresses in the soil under the pile cap are calculated using the formula:

$$p_1^{\max}(N) = \frac{p^{\max} \cdot AB - p_2^{\max}(N) \cdot ab}{(AB - ab)}$$
(14)

The stress in the cross section of the pile at the level of the head during cyclic loading is determined by the formula:

$$p_{2}^{max}(N) = \begin{cases} P \cdot G_{rp}(N) \cdot AB(AB - ab) \cdot L \cdot \beta_{gr} \left(1 - \frac{l}{L}\right) + \\ +0.33 \cdot \tau_{0}(N) \cdot E_{gr}(N) \cdot (A - a)(AB - ab) \cdot k_{1} + \\ +0.33 \cdot \tau_{0}(N) \cdot E_{gr}(B - b)(AB - ab) - \\ -4 \cdot \frac{\tau_{0}(N)}{\alpha} \cdot E_{gr}(N) \cdot l(AB - ab) \cdot \omega \left(1 - v_{gr}\right) \cdot k(l) + \\ + \frac{\tau_{0}(N)}{\alpha} \cdot E_{gr}(N) \cdot \frac{a+b}{b} \cdot l(AB - ab) \cdot \\ \cdot e^{-\alpha l} \cdot \omega \left(1 - v_{gr}\right) \cdot k(l) \end{cases}$$

$$\cdot \begin{bmatrix} a \cdot \omega \cdot \left(1 - v_{gr}\right) \cdot k(l) \cdot (AB - ab) \cdot E_{gr}(N) + \\ + ab \cdot \beta_{gr} \cdot L \cdot \left(1 - \frac{l}{L}\right) \cdot G_{gr}(N) \end{bmatrix}^{-1}$$

where G is the modulus of soil shear under cyclic loading; k(l) is a coefficient that takes into account the effect of the depth of the rigid stamp application; l is the length of the pile.

The stresses in the soil under the pile toe can be calculated using the formula:

$$p_3^{\max}(N) = \frac{p_2(N) \cdot 4ab + 4(a+b) \cdot l \cdot \frac{\tau_0(N)}{\alpha}}{4ab} - \frac{4(a+b) \cdot l \cdot \frac{\tau_0(N)}{\alpha} e^{-\alpha l}}{4ab}$$
 (16)

The bearing capacity of the subgrade soils of a raft-pile foundation under cyclic loading at the time (t = N), depending on the ratio  $\tau_0$   $(N) \le \tau^*(N)$ , is estimated based on the conditions for two zones:

- under the pile cap:

$$p_1^{max}(N) \le \sigma_{1u}(N) \tag{17}$$

- under the pile toe:

$$p_3^{max}(N) \le \sigma_{1u}(N) \tag{18}$$

where  $\sigma_{1u}$  (N) is the ultimate compressive stress in the soil under triaxial cyclic loading.

Ultimate stresses in the subgrade soil of a raft-pile foundation under triaxial cyclic loading are determined based on the calculation model of the soil under regime triaxial loading (Mirsayapov & Koroleva 2015).

The strength of the soil under cyclic triaxial compression depends on the change of friction angle, cohesion and ultimate equilibrium surface inclination angle.

According to the results (Mirsayapov & Koroleva 2014), failure occurs when the degree of damage by microcracks in ultimate equilibrium zone is critical. Soil strength reduction in time is mainly due to the cohesion forces decrease, whereas the friction angle chandes slightly.

In the initial stage of the long-time triaxial compression heterogeneity of stress-strain state in the soil sample is observed. Deviator loading and long exposures under regime deviator loading are accompanied by multiple shear surfaces emergence and development and soil sample discontinuities, the position of which changes in the process of deviator increasing and in time, and therefore, the negative dilatancy of clay soil (ripping) under long-term triaxial compression is localized in the zones of potential ultimate equilibrium surfaces (Mirsayapov & Koroleva 2014). Due to the fact that the soil ripping (dilatancy) in these local zones occurs in cramped conditions (constrained dilatancy) in the soil around the ripping area takes place a stress dilatancy. This area is a buffer zone of force transmission from the vertical pyramids area to undisturbed soil zone (Fig. 3). In the clay soil ultimate state destruction is localized in zones between compacted pyramids and at this stage in these zones it is possible to assume that the stress-strain state of the sample is homogeneous.

Based on the proposed model (Mirsayapov & Koroleva 2015) and the experimental results with the suggested scheme of clayey soils inelastic deformation long-term loading, according to which the strength of the Coulomb friction deviates from the limit equilibrium surface and acts in the surface of purely tangential sliding physical particles. Determination of such potentially hazardous orientation areas requires consideration of the soil deformed state.

Taking into consideration that, regardless of the heterogeneity of the soil elementary volume in initial stress-strain state, destruction always occurs in the space of principal stresses, combining the space of principal stresses  $\sigma_1$ ,  $\sigma_2$ ,  $\sigma_3$  and space principal strains  $\epsilon_1$ ,  $\epsilon_2$ ,  $\epsilon_3$  and preserving the principle of the coaxiality of stress and strain rate tensor (Mirsayapov & Koroleva 2015), we assume that the Coulomb friction law relates the forces projection acting on the ultimate equilibrium surface normal to the sliding platform and to itself. Then the condition of creep for long-term and cyclic loading can be presented as:

$$|t| = S \cdot tg\phi(t, t_1, N, \tau) + c_0(t, t_1, N, \tau), \tag{19}$$

where  $S = \sigma_1 \cdot l \cdot l + \sigma_2 \cdot m \cdot m' + \sigma_3 \cdot n \cdot n'$ ;  $t = ((\sigma_1 \cdot l \cdot m' - \sigma_2 \cdot m \cdot l')^2 + (\sigma_2 \cdot m \cdot n' - \sigma_3 \cdot n \cdot m')^2 + (\sigma_3 \cdot n \cdot l' - \sigma_1 \cdot l \cdot n')^2)^{1/2}$ ;  $\varphi(t, t_1, N, \tau)$  is the time-depend friction angle;  $c_0(t, t_1, N, \tau)$  is the time-depend cohesion; l, m, n – direction cosines of the normal to the limit equilibrium surface; l', m', n' – direction cosines of the normal to the sliding surface.

Spatial orientation of the ultimate equilibrium surface is determined by the formulas (Mirsayapov & Koroleva 2011):

$$l^2 = \frac{\bar{I}_3}{\bar{I}_2 \cdot \bar{\sigma}_1}; \quad m^2 = \frac{\bar{I}_3}{\bar{I}_2 \cdot \bar{\sigma}_2}; \quad n^2 = \frac{\bar{I}_3}{\bar{I}_2 \cdot \bar{\sigma}_3};$$
 (20)

where  $\bar{I_2} = \bar{\sigma_1} \cdot \bar{\sigma_2} + \bar{\sigma_2} \cdot \bar{\sigma_3} + \bar{\sigma_3} \cdot \bar{\sigma_1}$  and  $\bar{I_3} = \bar{\sigma_1} \cdot \bar{\sigma_2} \cdot \bar{\sigma_3}$  - second and third invariants of modified main stresses tensors  $\bar{\sigma_i} = \sigma_i + H$  (i = 1, 2, 3);  $H = c/\text{ctg}\phi$  - uniform compression defined by Mohr-Coulomb's hypothesis;  $\phi$  is the time-depend friction angle; c - time-depend cohesion under the regime long-term and cyclic loading.

Expressions for the directional cosines of normal of the sliding surfaces are presented as (Mirsayapov & Koroleva 2015):

$$(l')^{2} = \frac{1}{3} \cdot \frac{3 \cdot d\varepsilon_{2} \cdot d\varepsilon_{3} - l_{2} + \sqrt{l_{2}^{2} - 3 \cdot l_{1} \cdot l_{3}}}{(d\varepsilon_{1} - d\varepsilon_{2}) \cdot (d\varepsilon_{1} - d\varepsilon_{3})};$$

$$(m')^{2} = \frac{1}{3} \cdot \frac{3 \cdot d\varepsilon_{1} \cdot d\varepsilon_{3} - l_{2} + \sqrt{l_{2}^{2} - 3 \cdot l_{1} \cdot l_{3}}}{(d\varepsilon_{2} - d\varepsilon_{1}) \cdot (d\varepsilon_{2} - d\varepsilon_{3})};$$

$$(n')^{2} = \frac{1}{3} \cdot \frac{3 \cdot d\varepsilon_{1} \cdot d\varepsilon_{2} - l_{2} + \sqrt{l_{2}^{2} - 3 \cdot l_{1} \cdot l_{3}}}{(d\varepsilon_{3} - d\varepsilon_{1}) \cdot (d\varepsilon_{3} - d\varepsilon_{2})};$$

$$(21)$$

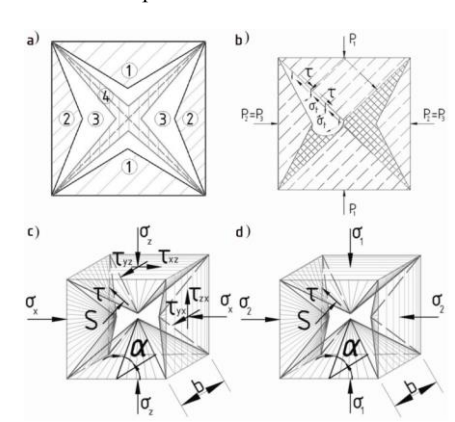
where  $d\varepsilon_1$ ,  $d\varepsilon_2$ ,  $d\varepsilon_3$  is the principal strain increments under the regime long-term and cyclic loading;  $I_1 = d\varepsilon_1 + d\varepsilon_2 + d\varepsilon_3$ ;  $I_2 = d\varepsilon_1 \cdot d\varepsilon_2 + d\varepsilon_2 \cdot d\varepsilon_3 + d\varepsilon_1 \cdot d\varepsilon_3$ ;  $I_3 = d\varepsilon_1 \cdot d\varepsilon_2 \cdot d\varepsilon_3$  – first, second and third deformation increments invariants.

As mentioned above, the potential sites [planes] of limit state orientation in general case is not constant, but changes during inelastic soil deformation under regime long-term and cyclic loading.

Based on the above described model and experimental results (Fig. 3) the condition of long-term bearing capacity under triaxial compression presented as:

$$4 \cdot \begin{bmatrix} \sigma_V(t, t_1, N) \cdot A_{sh} \cdot \cos \alpha_1(t, t_1, N) + \\ +\tau_V(t, t_1, N) \cdot A_{sh} \cdot \sin \alpha_1(t, t_1, N) \end{bmatrix} \ge \sigma_1 \cdot A_1, \quad (22)$$

Based on the results of studies (Mirsayapov & Koroleva 2014, Mirsayapov & Shakirov 2019) the following scheme for the creep deformation development and long-term destruction resistance changes during the cyclic loading can be presented. Depending on the value and duration of load in a multiphase clay soils two mutually offsetting effects occur - hardening due to defects healing and the thicker the particles recomposition, and the softening caused by the particles reorientation, cause of formation and development of micro- and macro-cracks (Fig. 3). In cases, where softening starts to prevail over the hardening, destruction and progressive creep stage occur. At this stage happens the intensive microstructure decay and the particles reorientation. These processes do not cover the entire soil volume, but only limit equilibrium zone with low resistance value, where the development of cracks occurs.



The equation showing the change in the cohesion:

$$c_0(t,\tau) = K_{lct}^M \cdot q(S), \tag{23}$$

where q(S) is the function of cracks total length S;  $K_{Ict}^{M}$  is the stress intensity factor at the crack top in the soil under the cyclic loading.

The critical crack length depends on the external load, Young modulus and soil destruction energy

After some transformations and simplifications we obtain the function of ground strength reduction (cohesion) under the regime loading:

$$\eta(t,\tau_1) = m(t,\tau_1) \cdot \lambda(t,\tau_1) \cdot \sqrt{\frac{K(\tau_1)}{K(t)} \cdot \frac{1}{1 + K(\tau_1) \cdot C(t,\tau_1)}}$$
 (24)

Then the cohesion between the particles, taking into account the factor of time is presented as:

$$C_{0}(t,\tau_{1}) = C_{0}(\tau_{1}) \cdot m(t,\tau_{1}) \cdot \lambda(t,\tau_{1}) \cdot \left[ \frac{K(\tau_{1})}{K(t)} \right]^{0.5} \cdot [1 + K(\tau_{1}) \cdot C(t,\tau_{1})]^{-0.5}$$
(25)

where  $C(t, \tau_l)$  is the soil volume creep rate;  $C_0(\tau_l)$  is the initial value of the soil cohesion under short-time loading;  $m(t, \tau_l)$  is soil hardening function due to recovery of water-colloidal bonds;  $\lambda(t, \tau_l)$  – hardening function by restoring the structural bonds of soil based on a combination of various blocks under the regime loading.

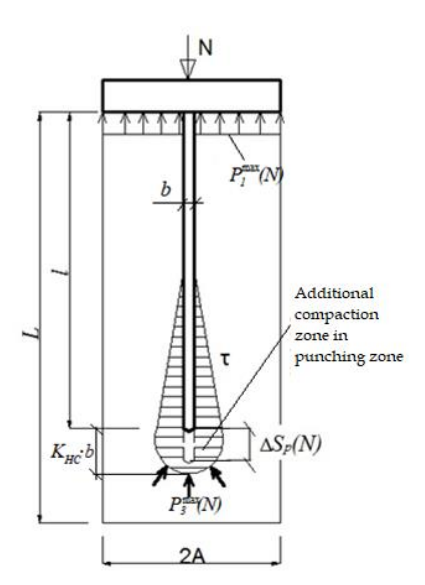
### 3 RESULTS

Thus, we consider the ultimate stress-strain state of the system "pile cap – pile - soil between pile space - soil below the toe of the pile". When a pile is rigidly connected to a pile cap, all elements of the system are deformed together during cyclic loading and forces are redistributed between them.

After a certain number of loading cycles, the stresses in the soil reach the endurance limit in one of the elements:

- under the pile cap and then after a certain number of cycles under the pile toe;
- under the pile toe;
- under the pile cap and the pile toe reaching together.

Then a thin layer of soil is pushed under the toe and, as a result, there is an increment in the movement (settlement) of the raft-pile foundation and this process is periodically repeated until the total settlement of the pile foundation reaches the limit value for a specific building or structure.



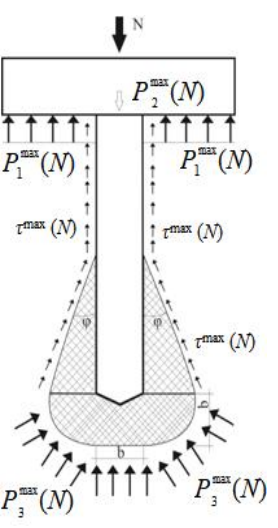


Figure 4. Design schemas of the pile-soil system for calculating the punching settlement.

The adopted design scheme of the system pile – soil function for the calculation of punching raft-pile foundations under cyclic loading (Fig. 4) is determined by the summation of the layers deformations by separation conditional depth into equal

$$\Delta S_n(N) = \sum_{i=1}^n K_{HC} \cdot \alpha_{CR} \cdot \varepsilon_{Zi}(N) \tag{26}$$

where  $K_{HC}(N)$  is a coefficient that takes into account the size of the punching zone at the maximum load of the cycle;

 $\varepsilon_z$  (N) is the relative vertical deformation of the soil in the area where the pile is pushed under the conditions of spatial stress in the i layer of the soil.

The relative axial vertical deformation in the soil in the area of pile punching is represented as:

$$\varepsilon_z(N) = \Delta \varepsilon_z = \frac{\Delta \sigma_z(N)}{G_v(N)} - \Delta \sigma_i(N) \frac{3K_v(N) - G_v(N)}{3K_v(N) \cdot G_v(N)}$$
(27)

where  $\Delta \sigma_z(N) = p_3^{max}(N)$  is the increment of vertical stresses in the soil under cyclic loading.

Intensity of stresses in the soil in the area of pile punching:

$$\Delta\sigma_i(N) = \frac{1}{\sqrt{2}} \sqrt{\frac{\left(\Delta\sigma_x - \Delta\sigma_y\right)^2 + \left(\Delta\sigma_y - \Delta\sigma_z\right)^2 + \left(\Delta\sigma_z - \Delta\sigma_x\right)^2 + 6\left(\tau_{xy}^2 + \tau_{yz}^2 + \tau_{zx}^2\right)}}$$
(28)

where  $\Delta \sigma_x = \Delta \sigma_y = P_3^{max}(N) \cdot \cos \varphi$ ;  $\Delta \sigma_z(N) = P_3^{max}(N)$ ;  $K_v(N) = \frac{\Delta \sigma^{max}(N)}{\Delta \varepsilon_v + \Delta \varepsilon_v(N)}$  conditional modulus of volume deformations;

 $G_v(N) = \frac{\Delta \sigma_i^{max}(N)}{3[\Delta \varepsilon_i + \Delta \varepsilon_i(N)]}$  conditional the shear modulus of the soil under triaxial compression;

 $\Delta \varepsilon_i(N)$ ,  $\Delta \varepsilon_i(N)$  is increment of volume deformations and strain intensity under cyclic loading.

Taking into account the above, the following sequence

- (algorithm) of the calculation is proposed:

  1. Determine the stresses  $\tau_0^{max}(N)$ ,  $p_1^{max}(N)$ ,  $p_2^{max}(N)$ ,  $p_3^{max}(N)$  based on equations (1-4) and taking into account (5-12), by the method of consecutive approximations according to formulas (13-16) in a various zones of the raft-pile foundation for a given number of loading cycles.
- 2. Determine the ultimate strength of the soil under triaxial cyclic loading from equation (22) for a given number of cycles.

- 3. Estimate the bearing capacity of the raft-pile foundation during cyclic loading based on the equations (17) and (18).
- 4. Calculate the intensity of stresses in the soil in the pile piercing area by formula (28).
- 5. Determine the relative axial vertical deformation in the soil in the pile junction area by formula (27).
- 6. Calculate the settlement of the raft-pile foundation for a given number of loading cycles based on equation (26) by summing the layers deformations when separating the conditional compressible depth to equal layers.

### 4 DISCUSSIONS

The regularities of changes in the stress-strain state of the soil under the pile toe of the raft-pile foundation under cyclic loading were established. A volumetric stress-strain state is realized in the considered zone.

The punching settlement of the raft-pile foundation under cyclic loading occurs when the maximum stress state is reached in two zones: in the soil under the pile cap and in the soil under the pile toe.

### 5 CONCLUSIONS

Performed analytical research has allowed establishing the main regularities of manifestation of the punching settlement of pile foundation under cyclic loading. According to them, the punching settlement is determined in step when the shear stresses on lateral surface missing in the upper and middle part of the pile due to reaching the ultimate shaft resistance. Punching settlement under the pile toe occurs when a pressure under the toe and under the pile cap exceeds the fatigue strength of the soil during cyclic triaxial compression.

Equations of the bearing capacity and punching settlement of raft-pile foundation under cyclic loading were developed. The obtained equations of the mechanical state of a raft-pile foundation describe the main regularities of the behavior of such foundations observed in experiments at various stages of loading and allow us to reliably estimate the settlement of raft-pile foundations under cyclic loading.

The calculation model that describes the development of pressure on the pile foundation has been developed. When comparing the calculation results with the experimental data (Mirsayapov & Shakirov 2016) of the pile cap model in laboratory and field tests, there is a good convergence between the calculated and experimental values (deviation of no more than 15%).

### 6 REFERENCES

- Bokov I. A., Fedorovskii V. G. 2018. On the Calculation of Groups of Piles Using Mutual Influence Coefficients in the Elastic Half-Space Model. Soil Mechanics and Foundation Engineering 54 (6), 363– 370.
- Bokov I. A., Fedorovskii V. G. 2019. On the Applicability of the Influence Function Obtained from Single-Pile Calculations for the Calculation of Pile Groups. Soil Mechanics and Foundation Engineering 55 (6), 359–365.
- Harichkin A. I., Shulyatev O. A., Kurillo S. V., Fedorovsky V. G. 2018. Features of interaction of piles with each other and with the soil as part of groups. Issues of design and construction of aboveground and underground structures of buildings and structures, 56-67.
- Hirai H. 2017. Assessment of cyclic response to suction caisson in clay using a three-dimensional displacement approach. Mar. Georesources Geotechnol 36 (7), 805–817.
- Lei H., Li B., Lu H., and Ren Q. 2016. Dynamic deformation behavior and cyclic degradation of ultrasoft soil under cyclic loading. J. Mater. Civ. Eng. 28 (11), 450.

- Mirsayapov I. T., Koroleva I. V., Ivanova O. A. 2012. Low-Cycle endurance and deformation of clay soils under three-axis cyclic loading. Housing construction in Moscow 9, 6–8.
- Mirsayapov, I.T., Koroleva, I.V. 2014. Computational model of the nonlinear deformation of clayey soils under complex stress state under regime loading. Soil-Structure Interaction, Underground Structures and Retaining Walls: Proceedings, International Scientific Conference on Geotechnical Engineering 57–64.
- Mirsayapov I. T., Koroleva I. V. 2015. Bearing capacity of foundations under regime cyclic loading. 15th Asian Reg. Conf. Soil Mech. Geotech. Eng., Fukuoka, Japan, 1214–1217.
- Mirsayapov Ilizar T., Shakirov M. I. 2016. Bearing capacity and settlement of raft-pile foundations under cyclic loading. *Izvestiya* KGASU 35 (1), 111-117.
- Mirsayapov Ilizar T., Shakirov M. I. 2019. Calculation settlement of the base of combined raft-pile foundations under cyclic loading. *Izvestiya KGASU* 4 (50), 255–262.
- Ni J., Indraratna B., Geng X.Y., Carter J. P., and Chen Y.L. 2015. Model of soft soils under cyclic loading. *Int. J. Geomech* 15 (4), 212.
- Ren X.-W., Xu Q., Teng J., Zhao N., Lv L. 2018. A novel model for the cumulative plastic strain of soft marine clay under long-term low cyclic loads. *Ocean Eng.* 149, 194–204.
- Shulyatev O. A. 2016. New set of rules for designing foundations and foundations of high-rise buildings. Soil Mechanics and Foundation Engineering 6, 37-40.
- Ter-Martirosyan Z. G., Sidorov V. V. 2010. Interaction of a long barreta with a single-layer and double-layer base. *Housing construction* 1, 36-39
- Travush V. I., Shulyatev O. A., Shulyatev S. O., Shakhramanyan A.M., Kolotovichev Yu. A. 2019. Analysis of the results of geotechnical monitoring of the Lakhta center tower. Soil Mechanics and Foundation Engineering 2, 15-21.